

eGastroenterology *ABCC2* p.R393W variant contributes to Dubin-Johnson syndrome by targeting MRP2 to proteasome degradation

Rong-Yue Sun,¹ Yi-Ming Chen,² Mian-Mian Zhu,¹ Ji-an Sun,¹ Hong-Wei Wang,³ Chen-Yu Wu,¹ Ting Zhu,¹ Yu-Jing Gong,¹ Chao-Sheng Lu,¹ Luisa Ronzoni,⁴ Luca Valenti,⁵ Ming-Hua Zheng ,⁶ Dan Wang ¹

To cite: Sun R-Y, Chen Y-M, Zhu M-M, *et al.* *ABCC2* p.R393W variant contributes to Dubin-Johnson syndrome by targeting MRP2 to proteasome degradation. *eGastroenterology* 2024;**2**:e100039. doi:10.1136/egastro-2023-100039

► Prepublication history and additional supplemental material for this paper are available online. To view these files, please visit the journal online (<http://dx.doi.org/10.1136/egastro-2023-100039>).

R-YS and Y-MC contributed equally.

Received 11 October 2023
Accepted 18 December 2023

ABSTRACT

Background Dubin-Johnson syndrome (DJS), a rare autosomal recessive liver condition, is caused by biallelic loss-of-function mutations of the *ABCC2* gene. This study aimed to investigate genetic variations in the drug efflux transporter *ABCC2* (MRP2) gene in patients with DJS and to characterise the expression and mechanism of the *ABCC2* gene variant.

Methods Trio whole exome sequencing was performed in the family to identify the genetic causes. Bioinformatics analysis was performed to assess pathogenicity. In *in vitro* experiments, site-directed mutagenesis was used to introduce *ABCC2* variants in constructs then expressed in HEK293T, HuH-7 and HepG2 cell lines. The expression of total and cell membrane MRP2 was quantified in cells expressing the wild-type or variant forms. Chloroquine and MG132 were used to evaluate the effects of p.R393W on lysosomal and/or proteasomal degradation.

Results The twin probands carry DJS-associated variants c.1177C>T (rs777902199) in the *ABCC2* gene inherited from the father and the c.3632T>C mutation in the other allele inherited from the mother. The *ABCC2* variant, c.1177C>T, results in a p.R393W substitution in MRP2 that is highly conserved among vertebrates, drastically decreasing the expression of mutant protein by promoting proteasomal degradation. Another variant c.3632T>C results in a p.L1211P substitution in MRP2, decreasing the expression of membrane MRP2 but not changing the expression of total protein.

Conclusion These results strongly suggest that the p.R393W variant affects the stability of the MRP2 protein and decreases its expression by ubiquitin-mediated proteasomal degradation, and the p.L1211P decreases the expression of membrane MRP2, indicating that these two variants, respectively, cause a loss-of-function of the MRP2 protein and membrane MRP2 ultimately leading to DJS development.

INTRODUCTION

Dubin-Johnson syndrome (DJS) is an autosomal recessive disorder characterised by intermittent or chronic conjugated hyperbilirubinaemia and liver pigmentation.¹ DJS occurs in all races and affects both sexes.^{2,3} This disease is caused by a deficiency

WHAT IS ALREADY KNOWN ON THIS TOPIC

⇒ Dubin-Johnson syndrome (DJS) is associated with *ABCC2* gene variants. *ABCC2* gene encodes multidrug resistance-associated protein 2 (MRP2). The *ABCC2* variants resulted in loss of function of the MRP2 protein.

WHAT THIS STUDY ADDS

⇒ In this work, we identified compound heterozygous variants c.1177C>T (p.R393W) and c.3632T>C (p.L1211P) in a DJS twin probands. Our *in vitro* results first showed that the *ABCC2* p.R393W variant affects the stability of the MRP2 protein by promoting its degradation via proteasomal pathway, and *ABCC2* p.L1211P variant decreases the expression of membrane MRP2, indicating that these two variants, respectively, cause a loss-of-function of the MRP2 protein and membrane MRP2 ultimately leading to DJS development.

HOW THIS STUDY MIGHT AFFECT RESEARCH, PRACTICE OR POLICY

⇒ Our study expands the genotypic spectrum of *ABCC2* variants of DJS and our understanding of the molecular mechanisms of this disease.

in non-bile acid organic anion transfer from hepatocytes to the canaliculus.^{1,4}

The human *ABCC2* (adenosine triphosphate-binding cassette subfamily C member 2) gene, located at chromosome 10q24, encodes the human MRP2 protein (multidrug resistance-associated protein 2), which localises on the hepatocytes' apical membrane and serves as a biliary transporter. It contains 17 transmembrane helices including three membrane-spanning domains (MSD) and two nucleotide-binding domains (figure 1A).⁴ MRP2 is a specific non-bile acid organic anion transporter that traffics from the endoplasmic reticulum to the canalicular membrane of hepatocytes, where it serves before recycling to the endosomal vesicles.⁴ As a biliary transporter, MRP2 promotes



© Author(s) (or their employer(s)) 2024. Re-use permitted under CC BY-NC. No commercial re-use. See rights and permissions. Published by BMJ.

For numbered affiliations see end of article.

Correspondence to

Dr Dan Wang;
wd608044@wmu.edu.cn

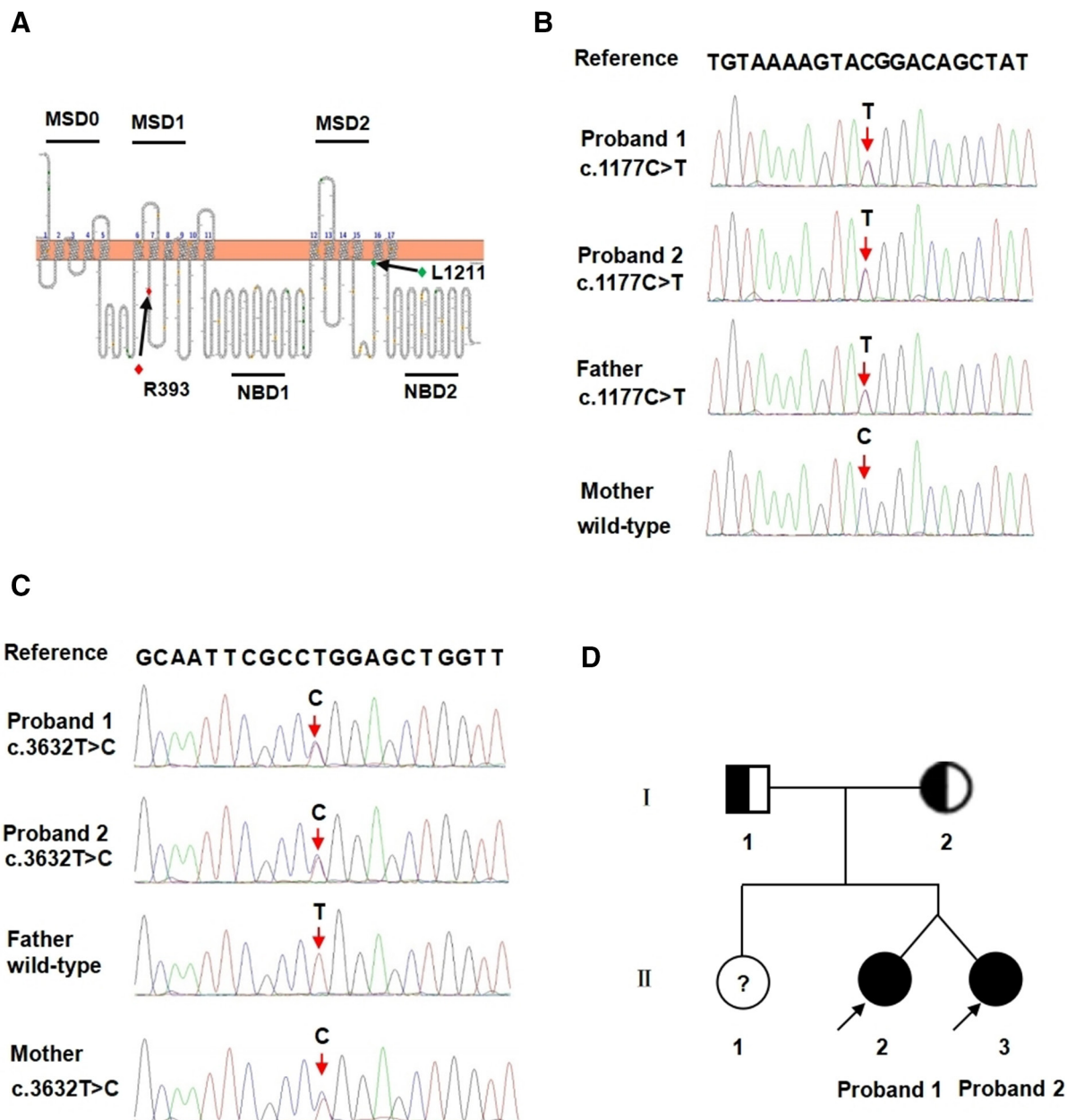


Figure 1 Topology model of MRP2 protein and pedigree of the studied family and the *ABCC2* exome sequencing results. (A) Localisation of the R393 and L1211 in a predicted topology model of MRP2 protein. The full-length model was generated by the open-source tool Protter (<http://wlab.ethz.ch/protter/start/>). (B) Sequencing analysis of the *ABCC2* gene indicates the disease-associated variant of probands (II-2, II-3), the missense mutation 1177C>T predicated to cause the mutation Arg393Trp (R393W) in the amino-acid sequence of the MRP2 protein heredity from the father (I-1) and (C) the missense mutation 3632T>C (L1211P) inherited from the mother (I-2). (D) Pedigree of the family presenting *ABCC2* variants. Circles and squares represent females and males, respectively. Half-black filled symbols represent heterozygous mutation carriers, and the question mark symbol indicates the normal subject without genetic examination. The black-filled symbols represent the twin probands. MSD, membrane-spanning domain; NBD, nucleotide-binding domain.

the ATP-dependent excretion of conjugate compounds including glutathione, sulfate and glucuronide into the canaliculi from the cytoplasm of hepatocytes.⁴

Genetic variations in *ABCC2* may alter transporter expression and be related to a variety of inherited and acquired cholestatic liver disorders.^{5–7} The pharmacokinetics and consequent pharmacological and toxicological drugs' effects may be altered by a malfunctioning transporter gene which determines the propensity of an

individual to develop hyperbilirubinaemia.^{8,9} Using candidate gene methodology, it was discovered in 1997 that the *ABCC2* gene is associated with DJS.¹⁰ By performing next generation sequencing in patients affected by DJS, several naturally occurring variants were found in *ABCC2* sequence, including exon skipping, nonsense, missense, small deletions or insertions, and splice site variations, causing truncated and dysfunctional MRP2.^{11–15} Previous studies have yielded initial insight into the mechanisms

by which DJS-causing variants in the *ABCC2* gene alter MRP2 function, resulting in the inhibition of bile acid excretion as well as ineffective transport of bilirubin out of hepatocytes.¹⁶ These findings are related to aberrant protein synthesis, and for missense variants to alter sublocalisation or secretory activity, which may cause MRP2 to remain in the endoplasmic reticulum rather than moving to the canalicular membrane, or finally to increased protein degradation.

The degradation of proteins in cells is a sophisticated and orderly process that ensures that proteins are constantly updated, including processing damaged and misfolded proteins, undesirable components, responding to upstream signals and degradation and protein synthesis from an amino acid cycle. The ubiquitin-proteasome system (UPS) and autophagy use proteasomes and lysosomes, respectively, as their primary proteolytic machinery for protein destruction in cells. UPS and autophagy are both necessary for the management of protein quality and quantity.¹⁷

Here, we report two cases of DJS in a 6-month-old dizygotic twin presenting with mild conjugated hyperbilirubinemia. Whole exome sequencing (WES) results indicated that the probands carried compound heterozygous variants in the *ABCC2* gene: the c.1177C>T (p.Arg393Trp, rs777902199, NM_000392.5) inherited from the father and the c.3632T>C (p.Leu1211Pro, NM_000392.5) inherited from the mother.

The variant c.3632T>C in *ABCC2* has not been reported before, we found that L1211P substitution could decrease the expression of membrane MRP2 but not change the expression of total MRP2 protein. However, rs777902199 has been reported correlated with DJS,^{18,19} we investigated its functional impact. We found that the R393 amino acid position, which is disrupted by this variant, is highly conserved among vertebrates and that the R393W substitution drastically decreased the MRP2 protein expression leading to an increase in proteasomal degradation, resulting in a more than 60% reduction in protein levels.

MATERIALS AND METHODS

Consent to participate

The probands with DJS and their family were enrolled from The First Affiliated Hospital of Wenzhou Medical University. Written informed consent for genetic analysis was obtained from both the parents.

WES and Sanger sequencing

We collected peripheral blood samples (3–5 mL) from the probands and their parents. Genomic DNA was extracted and purified using Genomic DNA Purification Kit (ThermoFisher Scientific, Waltham, Massachusetts, USA), and subsequently fragmented into random segments and captured using an Agilent Sure Select Human All Exome V6 Kit (Agilent Technologies, USA). WES was performed by in-solution hybridisation, followed by high-throughput paired-end sequencing on a NovaSeq 6000

platform (Illumina, San Diego, California, USA) which has a sensitivity of >99% to examine >95% of the target regions, with a reading length of 150 bp. Alignment to the GRCh37/hg19 human reference genome sequence was performed using a Burrows-Wheeler alignment tool (V.0.7.15). The gene variants were filtered and annotated using TGen (https://geneyx.com/geneyxanalysis/). The databases we used in this study include population databases (dbSNP, 1000G and gnomAD) and disease databases (UCSC, HGMD, OMIM, DECIPHER and ClinVar). According to the ACMG (American College of Medical Genetics and Genomics) guidelines, the pathogenicity of variants were classified into five categories: benign, likely benign, uncertain significance, likely pathogenic, pathogenic. Sanger sequencing was performed to validate the suspected variants in the probands and their parents. Primers were designed to amplify exon and intron boundaries by PCR. The products were sequenced using a 3500xL Genetic Analyzer (Applied Biosystems, Waltham, Massachusetts, USA).

In silico structural variant prediction assay

Public algorithms such as SIFT (http://sift.bii.a-star.edu.sg/), Polyphen2, REVEL, MutationTaster (http://www.mutationtaster.org/), CADD (https://cadd.gs.washington.edu/) and PROVEAN were used to assess variants pathogenicity. The topological model of the human MRP2 transporter was generated using the online tool Protter (http://wlab.ethz.ch/protter/start/). Secondary structures of the protein variants were predicted using NVOPRO (https://www.novopro.cn/tools/secondary-structure-prediction.html). The SWISS_MODEL (http://swissmodel.expasy.org/) was used to construct the three-dimensional structures of the protein variants. The splice mutation site was analysed with RDCC^{SC} (https://rddc.tsinghua-gd.org/).

Plasmids construction

A FLAG-*ABCC2*^{WT} plasmid expressing human *ABCC2* was purchased from Miaoling Bioscience (Wuhan, China). The cDNA of *ABCC2* was amplified by PCR and inserted into the pcDNA3.1-FLAG vector. The *ABCC2*^{WT} cDNA was used as a template to generate R393W and L1211P variants cDNA clone using the Mut Express II Fast Mutagenesis Kit V2 (Vazyme, Nanjing, China). All the plasmids were confirmed by sequencing. Primer sequences for generating R393W were as follows: forward: 5'-CAAGCTGG GTGTAAGATATGGACAGCTATCATGGCTTCTG-3' and reverse: 5'-CAGAAGCCATGATAGCTGTCCATA CTTTACACCCAGCTTGAAG-3'. Primer sequences for generating L1211P were as follows: forward: 5'-GTGG CTTGCAATTCGCCCGGAGCTGGTTGGGAAC-3' and reverse: 5'-GGTTCCTCAACCAGCTCCGGGCGAATTGC AAGCCACCTG-3'.

Cell culture, transfection and drug treatment

Human embryonic kidney (HEK293T) cells and human liver cancer cell lines, HuH-7 and HepG2, were obtained

from the American Type Culture Collection (Washington, DC, USA). The cell lines were cultured at 37°C with 5% CO₂ in Dulbecco's modified Eagle's medium, with 10% fetal bovine serum and 1% penicillin–streptomycin. According to the manufacturer's instructions of Lipofectamine 3000 (Glpbio Technology, Montclair, California, USA), cells were transfected with equal amounts pcDNA3.1-*ABCC2*^{WT}, pcDNA3.1-*ABCC2*^{R393W}. pcDNA3.1 was used as vector control. For further study, the transfected cells were treated with autophagy-lysosome pathway inhibitor chloroquine (CHL) (Glpbio Technology) at 100 µM for 24 hours before harvest, or ubiquitin-proteasome pathway inhibitor MG132 (Glpbio Technology) at 10 µM for the indicated time (0 hour, 2.5 hours, 5 hours, 10 hours, 20 hours) before harvest. For the half-life assay, equal amounts of HEK293T cells were transfected with equal amounts of pcDNA3.1-*ABCC2*^{WT} and pcDNA3.1-*ABCC2*^{R393W} plasmids. Cells were harvested for western blotting at 0, 2.5, 5 and 7.5 hours after treatment with 100 mg/mL cycloheximide (CHX).

Cell membrane protein isolation

Membrane protein was isolated using the Mem-PER Plus Kit (ThermoFisher Scientific). 5×10⁶ cells were scraped off the surface of the plate. The harvested cells were centrifuged at 300×g for 5 min, and the Cell Wash Solution was used to wash the cell pellet. The cytosolic and nuclear proteins were removed. The solubilised membranes and membrane-associated proteins were harvested and subjected to downstream applications.

Western blot analysis

Cells were harvested using ice-cold PBS and lysed in RIPA buffer with protease inhibitors (Tris-HCl, 50 mM; Triton X-100, 1%; deoxycholate, 1%; NaCl, 150 mM; and SDS, 10%). Protein concentration was determined using the Pierce BCA Protein Assay Kit (ThermoFisher Scientific). The cell lysates were separated on 10% Tris-glycine sodium dodecyl sulfate-polyacrylamide gel electrophoresis gels and transferred onto PVDF membranes. Primary antibodies against MRP2 (1:1000; Abcam, Cambridge, Massachusetts, USA) and FLAG-tag (1:7500; Sigma-Aldrich, St. Louis, Missouri, USA) were used for western blot analysis according to standard protocols. After incubation with horseradish peroxidase (HRP)-conjugated secondary antibodies (1:8000) for 1 hour at room temperature, Immobilon Western Chemiluminescent HRP Substrate (Thermo Fisher Scientific) was used to detect immunocomplexes on the membrane. Target protein band intensities were semiquantified and normalised to GAPDH (1:2000, Cell signaling Technology, Danvers, Massachusetts, USA) or Na⁺-K⁺-ATPase (1:1000, Cell signaling Technology).

Indirect immunofluorescence staining

HEK293T cells were transfected with equal amounts of pcDNA3.1-*ABCC2*^{WT}, pcDNA3.1-*ABCC2*^{R393W} or vector pcDNA3.1, respectively. Cells were cultivated in the

presence or absence of 10 µM MG132 for 24 hours. Then the cells were fixed using 4% paraformaldehyde for 20 min and blocked with blocking buffer (BSA) for 1 hour at room temperature. To detect MRP2 protein, cells were incubated with anti-MRP2 (1:300) as the primary antibody at 4°C overnight. After washing with phosphate buffered saline (PBS) three times, cells were incubated with DyLight 594 goat anti-rabbit IgG antibody (1:500; Jackson ImmunoResearch, Baltimore, Pennsylvania, USA) for 1.5 hours at room temperature. Finally, the immunofluorescence of the cells was observed and photographed by a confocal microscope (TCS SP8; Leica, Wetzlar, Germany).

Statistical analysis

At least three different runs of each experiment were completed. All data are expressed as mean±SD, and the unpaired Student's t-test followed by Welch's correction was used to compare the two groups. The criterion for statistical significance was p<0.05. GraphPad Prism .9.3 (San Diego, California, USA) was used to analyse the data.

RESULTS

Clinical characteristics of the DJS twins

The dizygotic female twin probands were born from non-consanguineous healthy parents after an uneventfully pregnancy obtained by *in vitro* fertilisation. Family history was unremarkable; the older sister was healthy. At the age of 6 months, a clinical diagnosis of DJS was suspected, based on biochemical evidences of direct hyperbilirubinaemia. Haemolysis, metabolic liver diseases, obstruction or dilation of the biliary tree, viral hepatitis and CMV infection, malignant tumours, and drug-induced or autoimmune liver diseases were ruled out. The clinical features of the twins are shown in online supplemental table 1. At the age of 6 months, total bilirubin and direct bilirubin were 94 µmol/L and 83 µmol/L in proband 1, and 62 µmol/L and 57 µmol/L in proband 2, respectively. The γ-glutamyl transpeptidase, total bile acid, alkaline phosphatase and albumin levels were within the normal range during follow-up to 2 years old. Aminotransferase levels elevated at 6 months, and gradually returned to normal at the age of 2 years. Blood and urine tandem mass spectrometry findings were normal. Abdominal ultrasonography revealed no obstruction or dilation of the hepatobiliary tract in either proband. Liver stiffness measured by FibroScan was 1.2 Kpa and 1.8 Kpa in proband 1 and proband 2 at the ages of 2 years, respectively.

WES revealed two rare missense variants in the *ABCC2* gene

WES analysis identified in both twins the same compound heterozygous variants of the *ABCC2* gene (figure 1B,C). The missense c.1177C>T variant (NM_000392.5), inherited from the father (I-1), substituted tryptophan to the conserved arginine at position 393 (p.R393W). The missense variant c.3632T>C (NM_000392.5), inherited from the mother (I-2), changed leucine to proline at position 1211 (p.L1211P) (figure 1D). Both parents

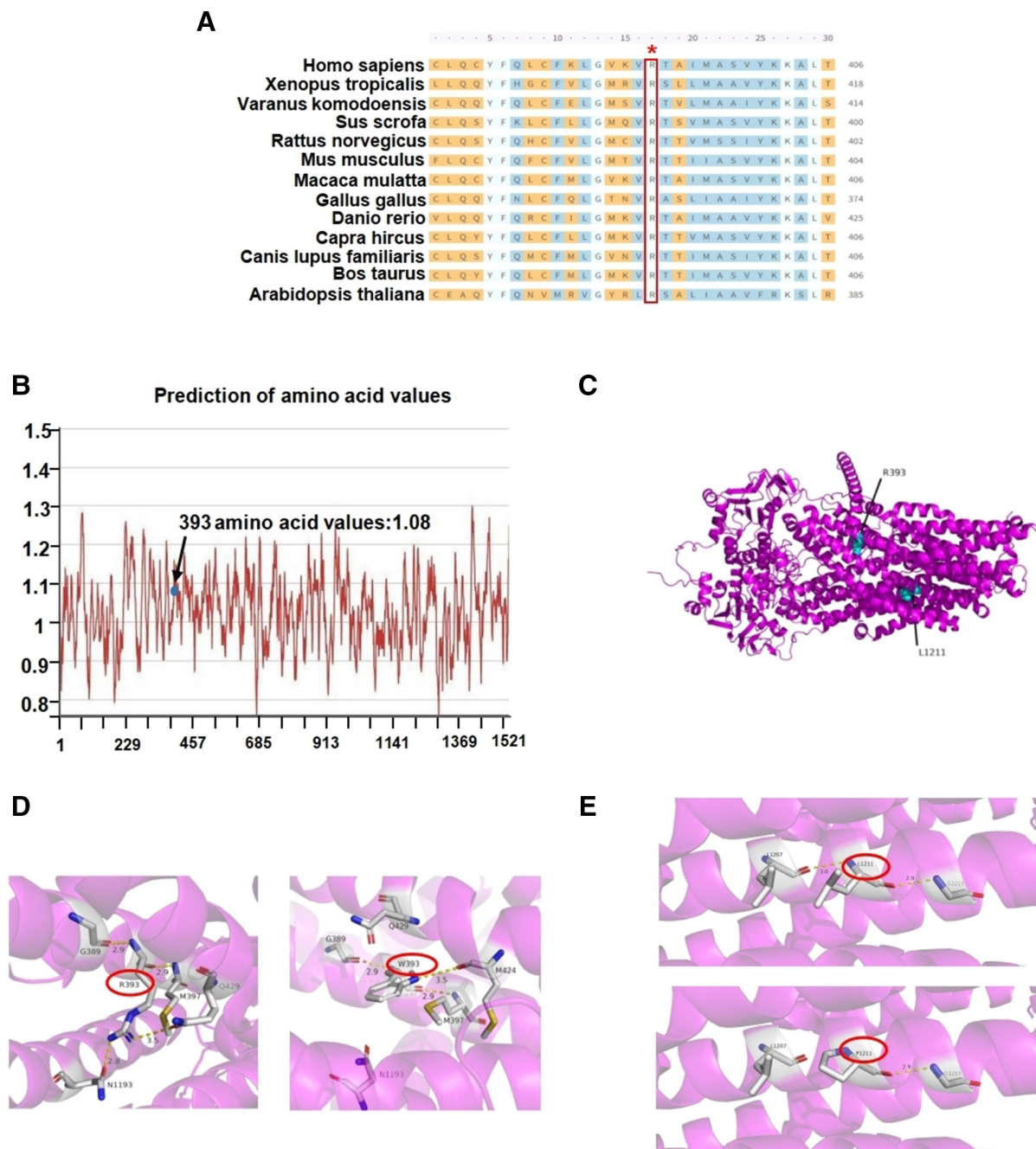


Figure 2 Results of in silico assay. (A) Alignment of multiple MPR2 protein sequences across species. The ABCC2 c.1177C>T resulted in an R393W substitution in MRP2 protein in the conserved amino acid region in different species. *Represents the position of the R393 is indicated by the red box. (B) Prediction of amino acid values. Arrow and blue dot indicate the position of R393. (C) Localisation of R393 and L1211 in MRP2 by SWISS_MODEL. (D) In wild-type MRP2 protein, R393 forms hydrogen bonds with G389, M397, Q429 and N1193. In mutant MRP2 protein, the hydrogen bond between W393 and Q429, and N1193 were broken, and a new hydrogen bond was formed between W393 and M424. (E) In wild-type MRP2 protein, L1211 forms hydrogen bonds with L1207 and G1215. In mutant MRP2 protein, the hydrogen bond between P1211 and L1207 were broken.

were heterozygous variant carriers. The p.R393W variant (rs777902199), already previously reported^{18 19}, was a rare variant with a minor allele frequency (MAF) of 0.00003 in the general population, according to public database (gnomAD), classified as Likely Pathogenic by ACMG guidelines and predicted as damaging or possible damaging by bioinformatic tools (online supplemental table 2). The p.L1211P was a novel variant not

previously described. Its MAF in the general population was unknown. Bioinformatic functional prediction demonstrated it was a damaging/possibly damaging variant (online supplemental table 2).

In silico structural variant prediction assay

To further investigate the possible effects of the missense variant c.1177C>T (p.R393W) on protein stability and

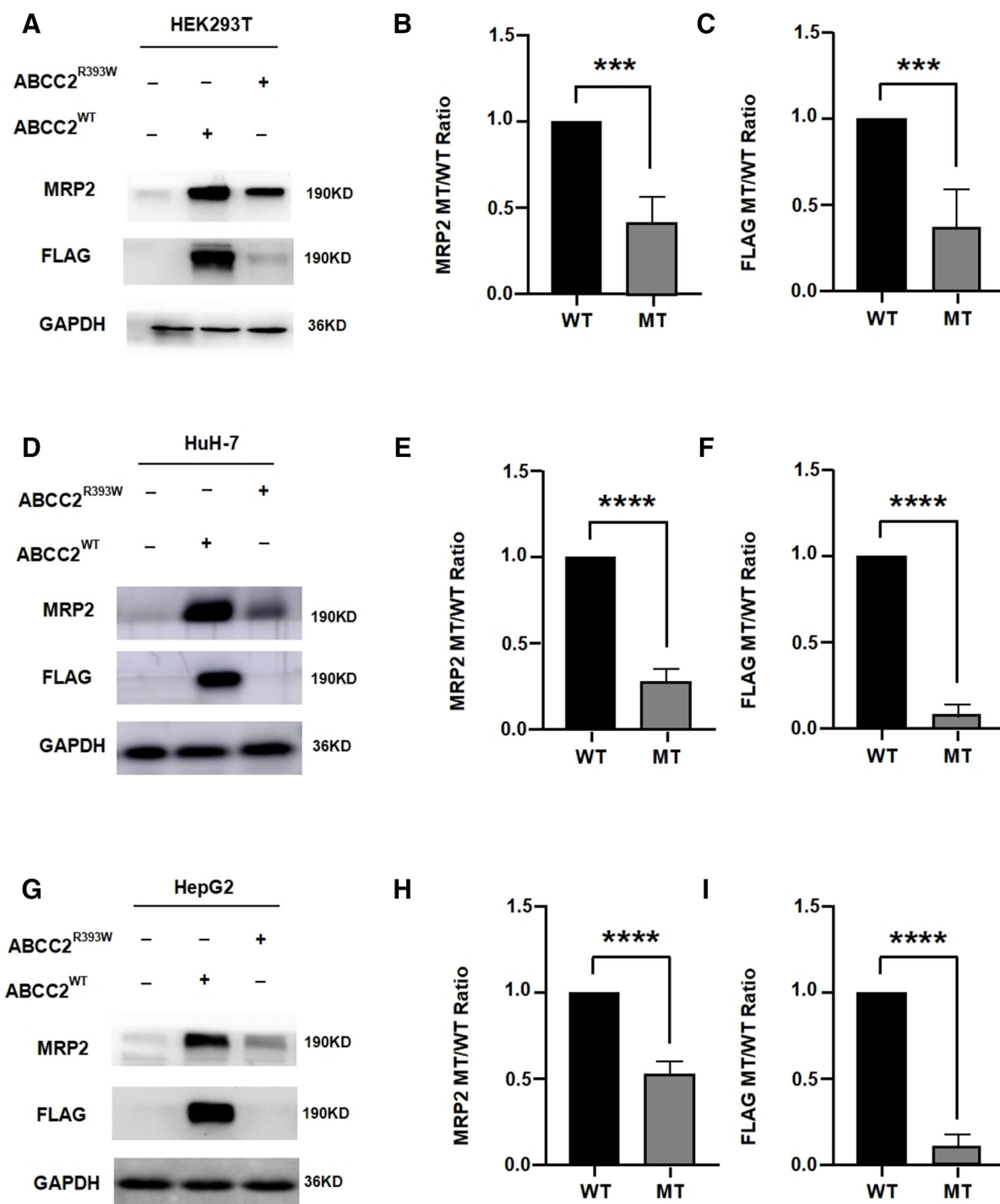


Figure 3 The protein expression of MRP2^{R393W} was decreased in three cell lines. Western blot bands and the quantification demonstrated that at equal transfection efficiency of pcDNA3.1-ABCC2^{WT}-FLAG and pcDNA3.1-ABCC2^{R393W}-FLAG in HEK293T (A–C), HuH-7 (D–F), and HepG2 (G–I) cell lines, the protein levels of overexpressed MRP2^{R393W} were significantly lower than that of MRP2^{WT}. All data are expressed as mean±SEM. Asterisks (*) represent statistically significant differences (**p<0.001, ****p<0.0001, n=3 replicates).

function, we performed *in silico* mutational modelling of the domains for which structural information was available. The missense variant c.1177C>T (p.R393W) was located in the MSD1 of MRP2 (figure 1A). Sequence comparison showed that amino acid 393 of MRP2 was conserved among vertebrate orthologs (figure 2A), and the prediction of amino acid values at position 393 is 1.08

at a high score (figure 2B). The 3D structure (figure 2C) visualised amino acid substitutions and locations in the functional domains of the MRP2 protein revealing that R393 was involved in hydrogen bonding with residues G389, M397, Q429 and N1193 (figure 2D), the L1211 involved in hydrogen bonding with residues L1207 and G1215 (figure 2E). The p.R393W variation removed

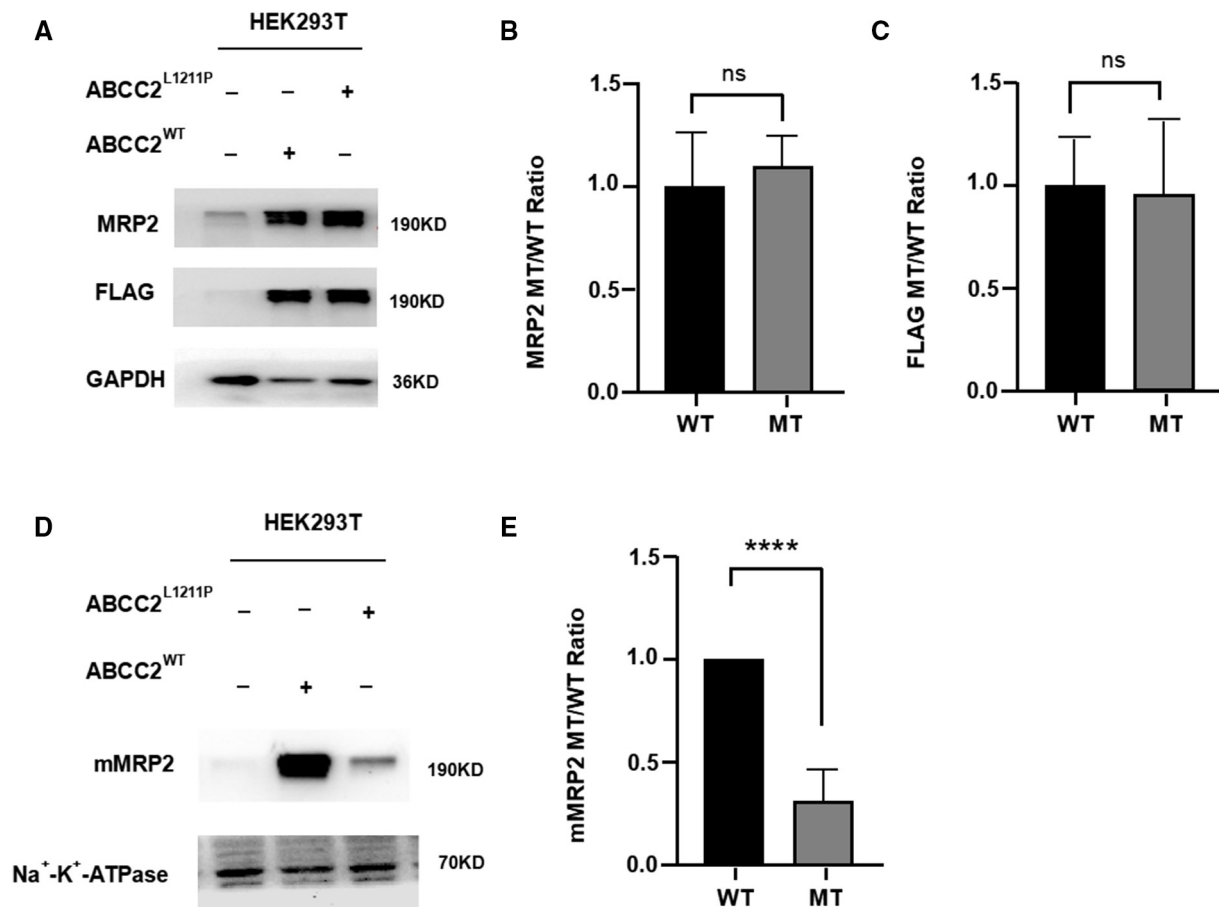


Figure 4 The total MRP2^{L1211P} protein level remains unchanged and membrane MRP2^{L1211P} was decreased. (A–C) Western blot bands and the quantification demonstrated that at equal transfection efficiency of pcDNA3.1-ABCC2^{WT}-FLAG and pcDNA3.1-ABCC2^{L1211P}-FLAG in HEK293T cell line, there is no difference in expression between MRP2^{WT} and MRP2^{L1211P}. (D, E) Expression of membrane MRP2 (mMRP2) was detected by cell fractionation and western blot. Na⁺-K⁺-ATPase was used as the loading control for cell membrane, the protein levels of mMRP2^{L1211P} were significantly lower than that of mMRP2^{WT}. All data are expressed as mean±SEM. Asterisks (*) represent statistically significant differences (****p<0.0001, n=3 replicates). ns, no significance.

all hydrogen bonds except M397 and created a new hydrogen bond with M424 (figure 2D). The hydrogen bond between P1211 and L1207 is broken in the p.L1211P variation (figure 2E). Because these two variants were in the functionally active sites of the protein, they might have harmful effects on MRP2 protein activity.

MRP2 protein expression was decreased in cell lines expressing mutant p.R393W_MRP2

Genomic *ABCC2* expresses a small amount of endogenous MRP2 protein. To investigate the effect of the p.R393W substitution on MRP2 synthesis, equal amounts of plasmids expressing wild-type (WT) or mutant c.1177C>T *ABCC2* were transfected into different cell lines: HEK293T, HuH-7 and HepG2. To ensure the accurate transient expression of *ABCC2*, the *ABCC2* gene was placed in front of three repeated FLAG tags. Western blotting revealed that the p.R393W_MRP2 (MRP2^{R393W}) protein levels were about 42%, 27% and 52% of WT_MRP2 (MRP2^{WT}) in HEK293T, HuH-7 and HepG2 cell lines, respectively (figure 3). The coexpressed FLAG-tag

showed that the protein levels were approximately 37%, 7% and 10% in these groups, respectively (figure 3).

The p.L1211P *ABCC2* variant does not change the expression of total MRP2 protein but decrease the expression of membrane MRP2

To investigate the effect of the p.L1211P substitution on MRP2 synthesis, equal amounts of plasmids expressing WT or mutant c.3632T>C *ABCC2* were transfected into HEK293T cell line. Western blotting revealed that the expression of MRP2^{L1211P} protein did not change in HEK293T compare to MRP2^{WT} (figure 4A–C). However, the results of membrane MRP2 (mMRP2) level displayed that the level of mMRP2^{L1211P} was reduced to 30% compared with mMRP2^{WT} (figure 4D,E).

The p.R393W *ABCC2* variant does not affect subcellular localisation

To investigate whether the *ABCC2*^{R393W} substitution leads to subcellular mislocalisation, we transfected HEK293T cells with FLAG-tagged *ABCC2* constructs and detected

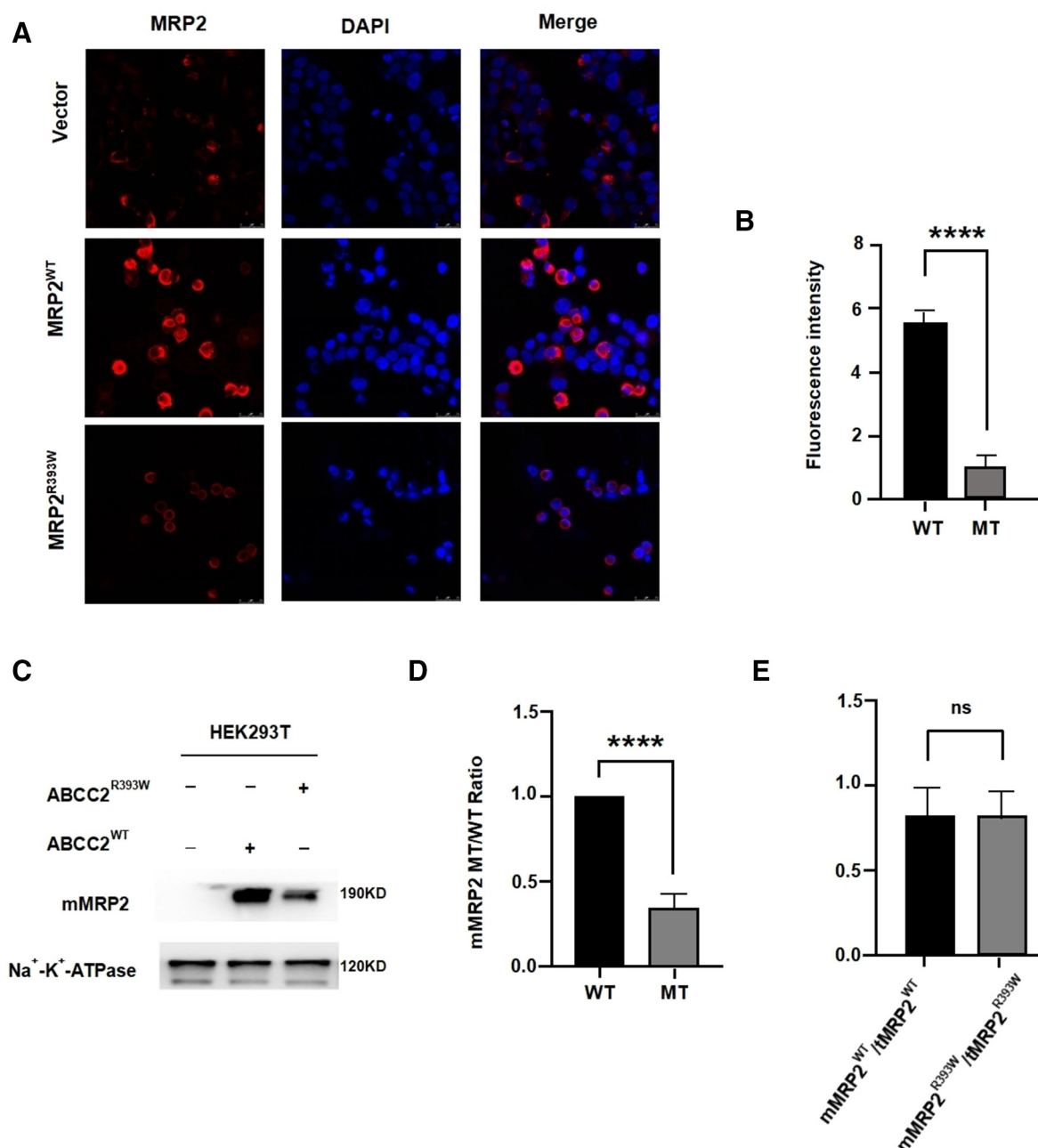


Figure 5 The subcellular localisation of MRP2^{R393W}. HEK293T cells were transfected with *ABCC2* wild-type or its variant plasmid. Empty pcDNA3.1 was vector control (A, B). Immunofluorescence assay showed the decreased MRP2^{R393W} expression both in cell membrane and cytoplasm. (C, D) Expression of membrane MRP2 (mMRP2) was detected by cell fractionation and western blot. Na⁺-K⁺-ATPase was used as the loading control for cell membrane. (E) The normalisation of mMRP2 to total MRP2 (mMRP2/tMRP2), total MRP2 protein images in figure 3A was used for normalisation. All data are expressed as Mean±SEM. Asterisks (*) represent statistically significant differences (****p<0.0001, n=3). ns, no significance.

the MRP2 protein by immunofluorescence analysis. The results of fluorescence showed that MRP2^{WT} localised to the cell membrane and cytoplasm, while the MRP2^{R393W} mutant was significantly reduced both in the cell membrane and cytoplasm (figure 5A,B). Cell fractionation was performed to further detect the membrane MRP2 (mMRP2) level: western blotting displayed that the level of mMRP2^{R393W} was reduced to 40% compared with mMRP2^{WT} (figure 5C,D). However, after normalising the total MRP2 (tMRP2) expression, the mMRP2^{R393W} did

not differ from mMRP2^{WT} (figure 5E), implying that the remarkable reduction of mMRP2^{R393W} might result from an overall decrease in MRP2^{R393W} protein levels.

The p.R393W substitution accelerated MRP2 degradation via the proteasomal pathway

We then explored the mechanism underlying the decrease of MRP2^{R393W} protein expression. RDDC^{SC} online analysis predicted that the p.R393W variant in *ABCC2* is unlikely to be involved in RNA splicing (online supplemental

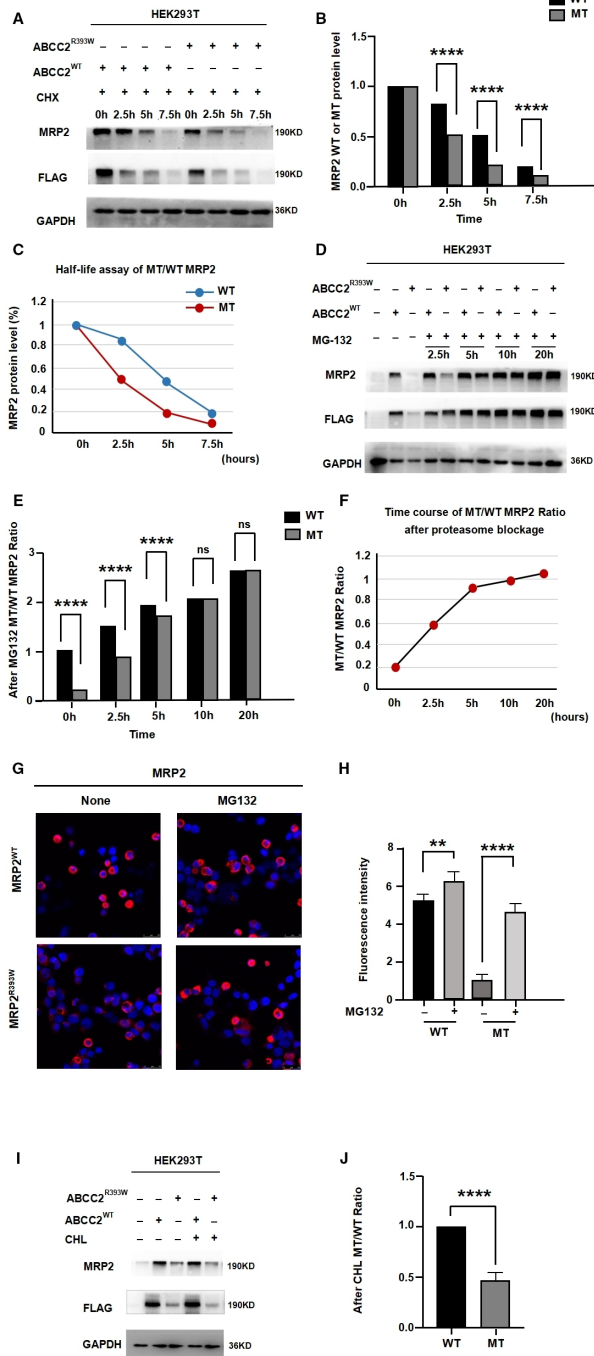


Figure 6 The p.R393W variant in MRP2 facilitated protein degradation via the proteasomal pathway. (A–C) Half-life assay of the MRP2^{WT} and MRP2^{R393W} by using cycloheximide (CHX) to block protein synthesis and chase the remaining protein level by western blot at 0, 2.5, 5 and 7.5 hours. The half-life of MRP2^{WT} was around 5 hours, whereas the MRP2^{R393W} was almost depleted within 2.5 hours. Western blot (D–F) and immunofluorescence (G, H) results of MRP2^{WT} and the MRP2^{R393W} expression after MG132 treatment indicated that proteasome blockage MG132 accumulated MRP2^{R393W} expression and attenuated the difference between the wild-type and mutant MRP2. (I, J) Whereas lysosome blockage chloroquine (CHL) failed to elevate the mutant MRP2 protein level. All data are expressed as mean±SEM. Asterisks (*) represent statistically significant differences (**p<0.01, ****p<0.0001, n=3 replicates). ns, no significance.

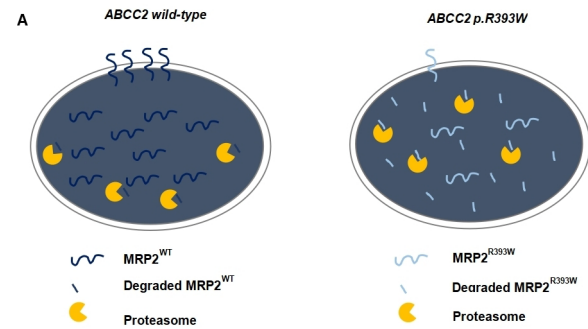


Figure 7 The pathogenic mechanism model of *ABCC2* p.R393W variant. (A) The p.R393W variant of *ABCC2* affects the stability of the MRP2 protein and promotes its degradation via proteasome pathway.

figure 1), implying that this variant may not alter the cDNA expression of *ABCC2*. Then, we treated HEK293T cells with cycloheximide to block protein synthesis. The half-life of MRP2^{WT} and MRP2^{R393W} were approximately 5 hours and 2.5 hours, respectively (figure 6A–C). The shorter half-life of MRP2^{R393W} indicates that p.R393W variant induces faster degradation than WT MRP2.

To further elucidate the degradation pathway of MRP2^{R393W}, HEK293T cells overexpressing either MRP2^{WT} or MRP2^{R393W} were treated with DMSO as a solvent control, the proteasome inhibitor MG132 for 0, 2.5, 5, 10 or 20 hours, or the lysosome inhibitor chloroquine (CHL) for 24 hours. MG132 significantly induced MRP2^{WT} and MRP2^{R393W} accumulation, and the protein levels of MRP2^{R393W} gradually elevated with prolonged treatment with MG132 (figure 6D–F). In contrast, CHL failed to accumulate MRP2^{R393W} protein (figure 6G,H). Figure 6I,J depicts the immunofluorescence images of HEK293T cells expressing MRP2^{WT} or MRP2^{R393W} that were incubated with or without 10 μM MG132 for 24 hours. After treatment, MRP2^{R393W} expression increased both in cell membrane and plasma. Taking together, these results demonstrated that the p.R393W *ABCC2* variant promoted MRP2 degradation via proteasomal pathway.

DISCUSSION

In the present study, we report the clinical manifestations of *ABCC2* variants in a dizygotic Chinese twin with DJS and we investigated the biological and functional consequences of the *ABCC2* variants c.1177C>T and c.3632T>C.

The probands exhibited the typical clinical presentation of conjugated hyperbilirubinaemia. Total bile acid and albumin levels were within the normal range during follow-up. Clinical symptoms and biochemical tests suggested a diagnosis of DJS. Actually, the diagnosis of DJS relies on clinical symptoms, liver histopathological manifestations or Sanger sequencing of the causative gene.²⁰ The average period between symptom onset and diagnosis is 13 years, indicating that DJS remains poorly understood and underdiagnosed¹¹; the low incidence and paucisymptomatic nature of the disease may explain this.

Because liver biopsies are invasive procedures, genetic testing is crucial for the early identification of DJS mainly in patients paucisymptomatic or with atypical presentations, such as newborn cholestasis.

In our study, WES revealed that both twin probands were compound heterozygotes for two variants in *ABCC2* gene: one (c.1177C>T; p.R393W), already previously described,¹⁸ derived from their father and the other one (c.3632T>C; p.L1211P), described here for the first time, from their mother. The parents, both carriers of a heterozygous variant and with a normal *ABCC2* allele to compensate for MRP2 functions, were healthy, as expected due to the autosomal recessive inheritance of DJS.

Although novel and diverse *ABCC2* variants are being rapidly uncovered by genetic analysis and found to be associated with MRP2 deficiency, the mechanisms by which genetic variants influence MRP2 expression remain unclear. Multiple mechanisms, including stability of the *ABCC2* mRNA,^{21 22} regulation of ATPase activity,²³ maturation and movement of MRP2 to the Golgi complex from the endoplasmic reticulum resulting in increased degradation of the MRP2 protein,^{24 25} interaction with microRNAs,²⁶ and susceptibility to ubiquitin-mediated proteasomal degradation²⁷ have been reported in previous studies.

MRP2 mainly localises in the canalicular or apical membrane of hepatocytes after synthesis in cellular plasma. A previous study showed the localisation of MRP2 protein was compromised by the p.G693R mutation of *ABCC2*.³ In our study, through functional assays, we demonstrated that mutant p.R393W MRP2 protein expression was significantly lower than that of WT and that the half-life of mutant MRP2 was shorter. We demonstrated that p.R393W substitution did not lead to subcellular mislocalisation, implying that the remarkable reduction of MRP2 expression in the cell membrane might result from an overall decrease in p.R393W MRP2 protein level; little is known about the underlying mechanisms. Autophagy and the ubiquitin-proteasome pathways play a significant role in maintaining protein levels in cells. We investigated the effect of MG132, an inhibitor of proteasomal proteolysis,²⁸ on the protein expression levels of the p.R393W variant in HEK293T cells; proteasome inhibition induced a significant time-dependent increase in MRP2 levels. In contrast, lysosomal inhibition by chloroquine did not affect protein levels. In conclusion, our cell-based experiments indicated that the p.R393W substitution (rs777902199) could decrease MRP2 expression by enhancing MRP2 degradation via the proteasome (figure 7). It is of great interest to understand how the inhibition of proteasomal protein degradation by MG132 to increasing the cells expressing the R393W variant protein, and this research can be carried out in the future. Also, we had not conducted *in vivo* animal experiments for validation, these were limitations in our research.

The other variant detected in the present study in *ABCC2*, c.3632T>C variant, resulted in an amino acid

substitution at the highly conserved position of L1211 in MRP2. Similar to the p.R393W variant, p.L1211P is a missense mutation located in the MSD2 domain of the MRP2 protein. Although this variant has not been previously described, *in silico* analysis predicted that this variant may be pathogenic. Functional study showed that p.L1211P resulted in decreased cell membrane MRP2 protein expression (figure 4).

CONCLUSIONS

In this study, we described dizygotic twin probands with DJS who were compound heterozygotes for two variants in *ABCC2* gene: c.1177C>T; p.R393W and the novel c.3632T>C; p.L1211P. Although we reported only one family, and more cases and additional studies are required, we proposed for the first time that the decrease in MRP2 protein levels, related to the p.R393W variants, was due to increased proteasomal degradation; the c.1177C>T variant leads to an amino acid substitution at the highly conserved position R393 of MRP2, decreasing protein stability and consequently increasing its degradation, significantly reducing the mutant protein levels. And the variant c.3632T>C could decrease membrane MRP2 protein expression. Moreover, with this study, we contributed to highlighting the role of genetic analysis, and particularly WES, for the diagnosis of DJS, mainly in patients with atypical or paucisymptomatic presentations.

Author affiliations

¹Department of Pediatrics, The First Affiliated Hospital Medical University, Wenzhou, Zhejiang, China

²Department of Hepatobiliary Surgery, The Second Affiliated Hospital and Yuying Children's Hospital Medical University, Wenzhou, Zhejiang, China

³Key Laboratory of Diagnosis and Treatment of Severe Hepato-Pancreatic Diseases, The First Affiliated Hospital Medical University, Wenzhou, Zhejiang, China

⁴Fondazione IRCCS Ca' Granda Ospedale Maggiore Policlinico, Milan, Italy

⁵Department of Pathophysiology and Transplantation, Università degli Studi di Milano, Milano, Italy

⁶MAFLD Research Center, Department of Hepatology, The First Affiliated Hospital Medical University, Wenzhou, Zhejiang, China

Acknowledgements The authors are grateful to the patients and their family for their understanding and cooperation, we thank Berry Genomics, for the technical support received.

Contributors DW and M-HZ conceived the study and designed experiments. R-YS, Y-MC and M-MZ conducted experiments. J-AS, C-YW and TZ collected the clinical information and data. Y-MC and H-WW performed the bioinformatic analysis. Y-JG and C-SL analysed the data. DW, M-HZ and R-YS interpreted the data. DW, M-HZ and R-YS wrote the manuscript. DW, M-HZ, LR and LV advised the structure and revised the manuscript. DW is responsible for the overall content as the guarantor. All authors read and approved the final manuscript.

Funding This work was supported by the National Natural Science Foundation of China (82171701), the Medical Science and Technology Project of Zhejiang Province (2022YK839), the Social Programs of Wenzhou Technology Bureau (2020Y0419, 2023Y0329) and the Zhejiang Medical Association (2020ZYC-B23).

Competing interests None declared.

Patient and public involvement Patients and/or the public were involved in the design, or conduct, or reporting, or dissemination plans of this research. Refer to the Methods section for further details.

Patient consent for publication Consent obtained from parent(s)/guardian(s).

Ethics approval This study involves human participants and the study was conducted in accordance with the Declaration of Helsinki and approved by the Ethics Committee (No. YS2022-686). Participants gave informed consent to participate in the study before taking part.

Provenance and peer review Not commissioned; externally peer reviewed.

Data availability statement Data are available on reasonable request.

Supplemental material This content has been supplied by the author(s). It has not been vetted by BMJ Publishing Group Limited (BMJ) and may not have been peer-reviewed. Any opinions or recommendations discussed are solely those of the author(s) and are not endorsed by BMJ. BMJ disclaims all liability and responsibility arising from any reliance placed on the content. Where the content includes any translated material, BMJ does not warrant the accuracy and reliability of the translations (including but not limited to local regulations, clinical guidelines, terminology, drug names and drug dosages), and is not responsible for any error and/or omissions arising from translation and adaptation or otherwise.

Open access This is an open access article distributed in accordance with the Creative Commons Attribution Non Commercial (CC BY-NC 4.0) license, which permits others to distribute, remix, adapt, build upon this work non-commercially, and license their derivative works on different terms, provided the original work is properly cited, appropriate credit is given, any changes made indicated, and the use is non-commercial. See: <http://creativecommons.org/licenses/by-nc/4.0/>.

ORCID iDs

Ming-Hua Zheng <http://orcid.org/0000-0003-4984-2631>

Dan Wang <http://orcid.org/0000-0003-2970-8400>

REFERENCES

- Memon N, Weinberger BI, Hegyi T, *et al*. Inherited disorders of bilirubin clearance. *Pediatr Res* 2016;79:378–86.
- Kim KY, Kim TH, Seong M-W, *et al*. Mutation spectrum and biochemical features in infants with neonatal Dubin-Johnson syndrome. *BMC Pediatr* 2020;20:369.
- Wu L, Li Y, Song Y, *et al*. A recurrent Abcc2P. G693R Mutation resulting in loss of function of Mrp2 and hyperbilirubinemia in Dubin-Johnson syndrome in China. *Orphanet J Rare Dis* 2020;15:74.
- Wen X, Joy MS, Aleksunes LM. In vitro transport activity and trafficking of Mrp2/Abcc2 polymorphic variants. *Pharm Res* 2017;34:1637–47.
- Zhou T-C, Li X, Li H, *et al*. Concurrence of novel mutations causing Gilbert's and Dubin-Johnson syndrome with poor clinical outcomes in a Han Chinese family. *J Hum Genet* 2023;68:17–23.
- Ontsouka E, Epstein A, Kallol S, *et al*. Placental expression of bile acid transporters in Intrahepatic cholestasis of pregnancy. *Int J Mol Sci* 2021;22:19.
- Huang YS, Chang TE, Perng CL, *et al*. The Association of transporter Abcc2 (Mrp2) genetic variation and drug-induced hyperbilirubinemia. *J Chin Med Assoc* 2021;84:129–35.
- Yang K, Battista C, Woodhead JL, *et al*. Systems pharmacology modeling of drug-induced hyperbilirubinemia: differentiating hepatotoxicity and inhibition of enzymes/transporters. *Clin Pharmacol Ther* 2017;101:501–9.
- Gini J, Olagunju A, Dickinson L, *et al*. Impact of Pharmacogenetics and pregnancy on tenofovir and Emtricitabine pharmacokinetics. *Pharmacogenomics* 2019;20:217–23.
- Paulusma CC, Kool M, Bosma PJ, *et al*. A Mutation in the human Canalicular Multispecific organic anion transporter gene causes the Dubin-Johnson syndrome. *Hepatology* 1997;25:1539–42.
- Corpechot C, Barbu V, Chazouillères O, *et al*. Genetic contribution of Abcc2 to Dubin-Johnson syndrome and inherited cholestatic disorders. *Liver Int* 2020;40:163–74.
- Wang N-L, Lu Y-L, Zhang P, *et al*. A specially designed multi-gene panel facilitates genetic diagnosis in children with Intrahepatic cholestasis: simultaneous test of known large insertions/deletions. *PLoS One* 2016;11:e0164058.
- Li M, Kong XY, Wang SM. Effects of splicing-regulatory Polymorphisms in Abcc2, Abcg2, and Abcb1 on methotrexate exposure in Chinese children with acute Lymphoblastic leukemia. *Cancer Chemother Pharmacol* 2023;91:77–87.
- Brandi G, Rizzo A, Deserti M, *et al*. Wilson disease, Abcc2 C.3972C > T polymorphism and primary liver cancers: suggestions from a familial cluster. *BMC Med Genet* 2020;21:225.
- Xiang R, Li J-J, Fan L-L, *et al*. Identification of a compound heterozygous Mutation of Abcc2 in a patient with hyperbilirubinemia. *Mol Med Rep* 2017;16:2830–4.
- Togawa T, Mizuochi T, Sugiura T, *et al*. Clinical, pathologic, and genetic features of neonatal Dubin-Johnson syndrome: A multicenter study in Japan. *J Pediatr* 2018;196:161–7.
- Wang X, Robbins J. Proteasomal and lysosomal protein degradation and heart disease. *J Mol Cell Cardiol* 2014;71:16–24.
- Machida I, Wakusawa S, Sanae F, *et al*. Mutational analysis of the Mrp2 gene and long-term follow-up of Dubin-Johnson syndrome in Japan. *J Gastroenterol* 2005;40:366–70.
- Wu L, Zhang W, Jia S, *et al*. Mutation analysis of the Abcc2 gene in Chinese patients with Dubin-Johnson syndrome. *Exp Ther Med* 2018;16:4201–6.
- Zhao C, Guan JX, Zhong B, *et al*. Clinical and pathological features of Dubin-Johnson syndrome. *Zhonghua Bing Li Xue Za Zhi* 2021;50:929–33.
- Laechelt S, Turrini E, Ruehmkoef A, *et al*. Impact of Abcc2 Haplotypes on transcriptional and Posttranscriptional gene regulation and function. *Pharmacogenomics J* 2011;11:25–34.
- Arlanov R, Porter A, Strand D, *et al*. Functional characterization of protein variants of the human multidrug transporter Abcc2 by a novel targeted expression system in Fibrosarcoma cells. *Hum Mutat* 2012;33:750–62.
- Elsens L, Tyteca D, Panin N, *et al*. Functional defect caused by the 4544G>A SNP in Abcc2: potential impact for drug cellular disposition. *Pharmacogenet Genomics* 2011;21:884–93.
- Hashimoto K, Uchiyama T, Konno T, *et al*. Trafficking and functional defects by mutations of the ATP-binding domains in Mrp2 in patients with Dubin-Johnson syndrome. *Hepatology* 2002;36:1236–45.
- Hirouchi M, Suzuki H, Itoda M, *et al*. Characterization of the cellular localization, expression level, and function of SNP variants of Mrp2/Abcc2. *Pharm Res* 2004;21:742–8.
- Werk AN, Bruckmueller H, Haenisch S, *et al*. Genetic variants may play an important role in mRNA-miRNA interaction: evidence for haplotype-dependent downregulation of Abcc2 (Mrp2) by miRNA-379. *Pharmacogenet Genomics* 2014;24:283–91.
- Furukawa T, Wakabayashi K, Tamura A, *et al*. Variant of human ABC transporter Abcg2 undergoes lysosomal and Proteasomal degradations. *Pharm Res* 2009;26:469–79.
- Guo N, Peng Z. Mg132, a Proteasome inhibitor, induces apoptosis in tumor cells. *Asia Pac J Clin Oncol* 2013;9:6–11.